ULTRAFAST OPTOELECTRONIC DEVICES FOR MILLIMETER-WAVES

C-1

Chi H. Lee, Aileen M. Vaucher, M. G. Li, and C. D. Striffler
Electrical Engineering Department
University of Maryland
College Park, Maryland 20742

We discuss a new class of devices in which the propagation parameters of millimeter-waves are controlled by a laser induced electron-hole plasma in a semiconductor waveguide. The performance of high speed (better than one nanosecond), efficient millimeter-wave phase shifters, modulators, switches, and gating devices are reported.

Introduction

To realize an electronically controllable phase array system in the millimeter-wave region, one requires a large number of switches and phase shifters[1] which can be operated with high speed (~one nanosecond) and with a time precision of several picoseconds. Such kinds of phase shifters, switches, and modulators are currently not available,[2] yet there is a great need to develop these types of devices. In this paper, we present the results of theoretical and experimental studies of a new class of devices in which the propagation parameters of the millimeter-wave signals are controlled by a laser induced electron-hole plasma in a semiconductor waveguide.[3]

It is well known that the complex dielectric constant of a semiconducting medium can be modified by the introduction of an optically induced electron-hole plasma. When the dimension of the plasma region is much smaller than the wavelength of the propagating rf signals, the plasma region may be regarded as a lumped circuit element. This leads to the usual photoconductivity effect. On the other hand, if the wavelength of the rf signals is comparable to or smaller than the dimension of the plasma region, the plasma region must be treated as a distributed circuit element. This is the situation that is discussed in this paper. Here the laser induced plasma causes a change both in refractive index and extinction coefficient, resulting in a phase shift and attenuation for millimeter-waves.

Shown in Fig. 1 is a schematic of the optically controllable millimeter-wave device. It consists of a rectangular semiconductor waveguide with tapered ends to allow efficient transition of millimeter-waves both to and from a conventional metallic waveguide. Optical control is realized when the broad wall of the semiconductor waveguide is illuminated by picosecond laser pulses.

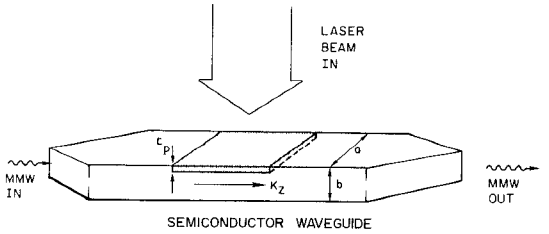

Fig. 1. Schematic diagram and operating principle of an optically controlled millimeter-wave waveguide device. K_z is the propagation vector in the guide, t_p is the depth of the injected plasma layer, and a and b are the width and height of the guide respectively.

Model and Analysis of a Plasma Controlled Dielectric Waveguide

The model of the rectangular dielectric-plasma guide for the purposes of theoretical analysis is shown in Fig. 2. The dimensions of the guide are a and b and the plasma region thickness is t_p. The relative dielectric constant and refractive index of the dielectric region, $0 < y < b-t_p$, are ε_r and $n_r = \sqrt{\varepsilon_r}$, respectively, and those of the dielectric plasma region, $b - t_p < y < b$, are[4]

$$\varepsilon_p = n_p^2 = \varepsilon_r - \sum_\alpha \frac{\omega_{p\alpha}^2}{\omega^2+\nu_\alpha^2} - j \sum_\alpha \frac{\omega_{p\alpha}^2}{\omega^2+\nu_\alpha^2} \frac{\nu_\alpha}{\omega} \equiv (\eta - j\kappa)^2. \quad (1)$$

The free charge contribution (plasma) is characterized by a plasma frequency $\omega_{p\alpha}=(q_\alpha^2 N_\alpha/m_\alpha \varepsilon_o)^{1/2}$ of each species of density N_α and an effective collision frequency ν_α. These various species in an optically formed plasma are denoted by thermally ionized and photoinduced holes (light and heavy) and electrons.

For the case of well guided modes, the analysis is considerably simplified in that the dispersion equation is essentially decoupled between the x and y directions.[5] That is, assuming the fields vary as $\exp i(\omega t - k_x x - k_y y - k_z z)$, then the boundary conditions in x determine k_x, those in y determine k_y, and from these one can then determine k_z. The modes decouple into TM modes, called $E^y_{p,q}$, and TE modes called $E^x_{p,q}$. The propagation constant k_z is computed for the cases with and without the presence of the plasma region, k_z' (complex), k_z(real), respectively, and from these the plasma induced phase shift $\Delta\phi$ for a given length of waveguide ℓ can be computed by

$$\Delta\phi = (\mathrm{Re}k_z' - k_z)\ell, \text{ radians} \quad (2)$$

and the attenuation coefficient by

$$\alpha = \mathrm{Im}k_z', \text{ cm}^{-1}. \quad (3)$$

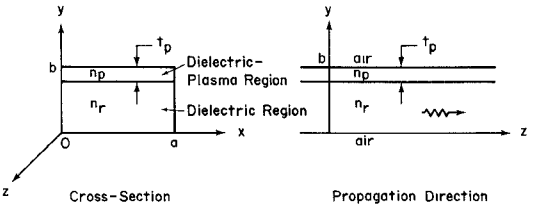

Figure 2 - Model of the dielectric-plasma waveguide

For the TM modes, $E^y_{p,q}$, the solution for k_x is[4]

$$k_x = \frac{p\pi}{a}\left[1 + \frac{1}{\pi a}\frac{\lambda_o}{(\varepsilon_r - 1)^{\frac{1}{2}}}\right]^{-1} \quad (4)$$

where p is the number of extrema in the x direction and λ_o is the free space wavelength of the propagating wave. The solution for k_y is found by solving

$$\tan^{-1}\frac{K_a \varepsilon_r}{k_r} + \tan^{-1}\left\{\frac{k_p}{k_r}\frac{\varepsilon_r}{\varepsilon_p}\tan\left[\tan^{-1}\left(\frac{K_a \varepsilon_p}{k_p}\right) - k_p t_p\right]\right\}$$

$$-k_r(b - t_p) + (q - 1)\pi = 0 \quad (5)$$

where q is the number of extrema in y, and the various values of k_y in each region are represented by,

0149-645X/83/0000-0187 $01.00 © 1983 IEEE

$$K_a = \frac{2\pi}{\lambda_o} (n_\omega^2 - 1)^{1/2},$$

$$k_r = \frac{2\pi}{\lambda_o} (n_r^2 - n_\omega^2)^{1/2},$$

$$k_p = \frac{2\pi}{\lambda_o} (n_p^2 - n_\omega^2)^{1/2},$$

and n_ω is the effective refractive index of the wave. In the plasma layer, the index n_p is complex and depends upon the density of the plasma [see Eq. (1)]. Equation (5) is numerically solved for n_ω, from which k_r is determined. We then calculate k_z' from

$$k_z' = (n_r^2 \frac{\omega^2}{c^2} - k_x^2 - k_r^2)^{1/2},$$

and then compute the phase shift $\Delta\phi$ and attenuation α via Equations (2) and (3).

As an example of the results obtained from the model we consider a Si waveguide of 2.4 x 1.0 mm^2 cross section and a plasma thickness of 10 μm. The phase shift and attenuation for this guide at 94 GHz is shown in Fig. 3 as a function of the plasma density. In Fig. 3a, the phase shift per centimeter is plotted for the $E^y_{1,1}$ through the $E^y_{5,1}$ modes which are the only $E^y_{p,1}$ modes that can propagate in this guide. The corresponding loss in dB/cm is plotted in Fig. 3b. As the plasma density increases from 10^{15} cm^{-3} to 10^{20} cm^{-3}, the skin depth in Si decreases from more than 200 μm to less than 1 μm. When the skin depth is equal to or larger than the plasma layer thickness, the millimeter wave penetrates deeply into the plasma layer causing loss. The maximum loss occurs when the skin depth is about equal to the layer thickness. The higher order modes have more loss in this regime than the lower order modes, because more of the wave power is concentrated in the plasma region. As the plasma density increases further, the skin depth decreases. When the skin depth is less than the thickness of the plasma layer, the plasma region begins to act as a metallic conductor and the dielectric waveguide becomes an image line. The attenuation then drops off rapidly with increasing plasma density. The maximum phase shift of the higher order modes is larger than that of the lower order modes because the waveguide becomes more dispersive closer to cutoff. The other two TM modes this guide is capable of supporting at 94 GHz are the $E^y_{1,2}$ and $E^y_{2,2}$ modes, both of which are of higher order than the $E^y_{5,1}$ mode. Their maximum phase shifts are 1000°/cm and 1450°/cm respectively.

Other results obtained for the guide are:

The phase shift and attenuation properties for TE modes, $E^x_{1,1}$ through $E^x_{4,1}$, are similar to those found for the $E^y_{p,q}$ modes, except that the magnitude of the maximum phase shift is less and the maximum loss in the guide is less, reflecting the different field distribution. The effect of varying the frequency of the millimeter wave is to shift the attenuation peak and the onset of the phase shift. This is to be expected since the skin depth is a decreasing function of frequency; therefore, the plasma density at which the greatest amount of interaction between the plasma and the wave occurs increases as frequency is increased. Also, as the frequency is lowered, the maximum phase shifts and attenuations are larger. This is because the guide operates closer to cutoff at the lower frequencies. For a frequency of 50 GHz, only one mode $E^y_{1,1}$, can propagate. For the same size GaAs guide the features with respect to multi-mode and frequency variation are similar to those presented for Si. The curves are shifted toward lower plasma densities consistent with the shift in the dielectric properties of GaAs versus Si.

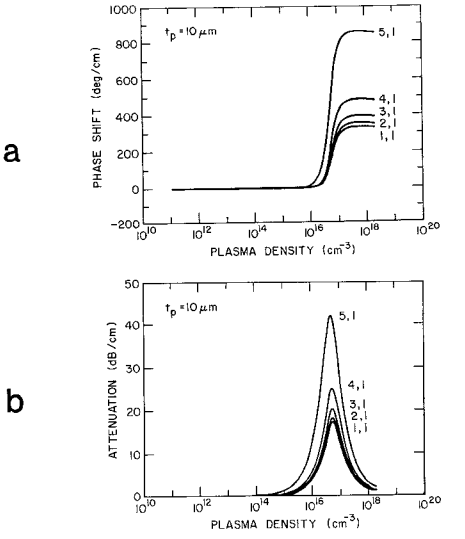

Figure 3 - Phase shift and attenuation properties in a 2.4 x 1.0 mm^2 Si waveguide at 94 GHz with respect to plasma density for a plasma region thickness of 10 μm. Parametric dependence is the TM mode, $E^y_{p,q}$. Si properties at 94 GHz are given in reference 3.

Experimental Results

We have successfully demonstrated the concept of optically controlled millimeter wave devices.[3,6,7] Millimeter-wave phase shifters at 94 GHz have been constructed. A millimeter-wave bridge similar to that used by Jacobs and Chrepta[1] was employed. A schematic diagram of the experimental arrangement is shown in Fig. 4. Measurements of the phase shift and attenuation were performed first by omitting the semiconductor waveguide outside the bridge in the figure. Initially, without laser illumination of the semiconductor waveguide, the bridge was balanced by adjusting the variable attenuator A and the mechanical phase shifter ϕ in arm b so that there was no signal at the output. When a single .53 μm pulse from a frequency doubled mode-locked Nd:YAG laser illuminated the semiconductor waveguide, a high-density electron-hole plasma was generated at the surface, causing phase shift and attenuation of the millimeter-wave signal as it propagated through the plasma covered region of the waveguide. The bridge became unbalanced and a signal appeared at the output. This signal persisted until the excess carriers recombined. Phase shifts of 300°/cm are observed from a Si waveguide with a cross-section of 2.4 x 1.0 mm^2 and 1400°/cm from a GaAs waveguide with a cross-section of 2.4 x 0.5 mm^2. These values are in good agreement with theoretical predictions.

Using the experimental setup depicted in Fig. 4 with both semiconductor waveguides made of Si it is possible to produce gated millimeter-wave signals. Initially the bridge is balanced, then a 0.53 μm pulse from a frequency doubled Nd:YAG laser is used to illuminate the waveguide inside the bridge. Because the recombination time in Si is of the order of microseconds, this signal will persist. To "turn off" the millimeter-wave pulse, a 1.06 μm pulse from the Nd:YAG is used to illuminate the Si waveguide outside the bridge. At this laser wavelength carriers are generated throughout

the bulk Si waveguide and the millimeter-waves are not allowed to propagate. By adjusting the delay between the two laser pulses millimeter wave pulses of desired duration may be obtained. The pulse repetition rate for this technique is limited to less than 1 MHz by the recombination rate in Si.

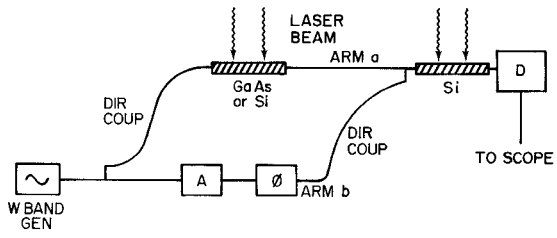

Figure 4 - Experimental arrangement

Replacing the Si waveguide inside the bridge with a waveguide made of Cr-doped GaAs increases the pulse repetition rate to greater than 200 MHz. Indeed, since the lifetime of the excess carriers is of the order of 100 ps in GaAs,[8] it is possible to produce short millimeter-wave pulses without using the Si waveguide outside the bridge to "turn off" the millimeter-wave signal. In fact, if an optical pulse train is used to illuminate the GaAs waveguide, a millimeter-wave pulse train mimicking the optical pulse train results. An oscilligram of the millimeter-wave pulse train is shown in Fig. 5. The interpulse spacing of 7 ns in the millimeter-wave pulse train is the same as that in the optical pulse train. Fig. 5 also shows that a modulation bandwidth approaching 1 GHz is attainable. The pulsewidths of the individual pulses are not resolvable in this figure since the combined response time of the detecting and display system is slower than the expected pulsewidth estimated on the basis of the carrier lifetime data.[8]

To measure the pulsewidth a correlation technique was used. Referring again to Fig. 4, a .53 μm pulse from a frequency doubled Nd:YAG laser was used to illuminate the GaAs waveguide inside the bridge, producing a millimeter-wave pulse. A 1.06 μm pulse from the laser was used to illuminate the Si waveguide outside the bridge and "turn off" the millimeter-wave signal. As the relative delay between the two optical pulses was varied, the integral of the millimeter-wave pulse with respect to time appeared at the detector. By taking the derivative, the millimeter-wave pulse width could be determined. Plots of the integrated signal and the pulse are given in Fig. 6. The millimeter-wave pulsewidth determined by this technique was 700 ps, wider than the expected pulsewidth by a factor of three. This discrepancy can be resolved by noting that the "turn off" of the millimeter-wave signal was not instantaneous and by realising that the millimeter-wave pulse is generated by rapid phase modulation of the signal. The rapid phase modulation of the signal causes the millimeter-wave pulse to be 'chirped', i.e., there is a large frequency sweep within the pulse. As the millimeter-wave pulse propagates in a positively dispersive guiding structure, group velocity dispersion will broaden it. Mismatches between the dielectric and metallic waveguides will also contribute to some broadening. Taking these effects into account, the actual pulsewidth of the millimeter-wave pulse is estimated to be 400 ps.

A dynamic bridge method has been developed in this study to monitor the dynamic phase shift and attenuation over a wide range of carrier density. A two component carrier decay with τ_1 = 100 ps and τ_2 = 1000 ps respectively has been observed in Cr-doped GaAs.

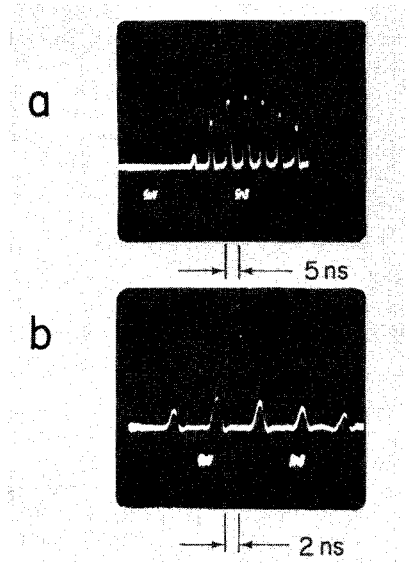

Fig. 5 - Millimeter-wave pulse train mimicking the incident optical pulse train. Individual pulse in train is "chirped" and its duration is measured by a correlation technique to be about 700 ps.

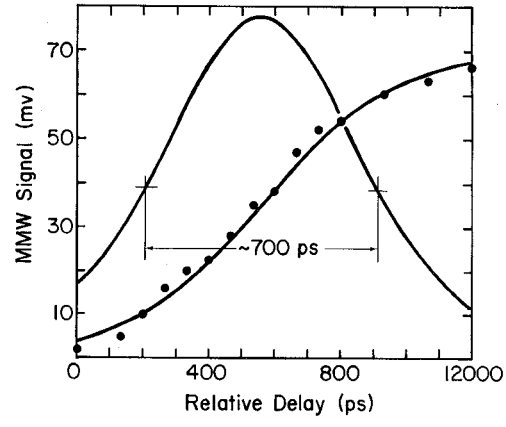

Fig. 6 - Plots of the integrated millimeter-wave signal (data points) and the millimeter-wave pulse.

Acknowledgement This work was supported in part by the Harry Diamond Laboratory, the U. S. Army, the Minta Martin Aeronautical Research Fund, College of Engineering, University of Maryland, and the University of Maryland Computer Science Facility.

References

1. H. Jacobs and M. M. Chrepta, IEEE Trans. MTT-22 pp. 411-417(1974).
2. T. Itoh, Ch. 5, Infrared and Millimeter-Waves, Vol. 4 Millimeter-Wave Systems, Ed. K.J.Button,J.C. Wiltse, Academic Press (1981).
3. Chi H. Lee, P.S. Mak, and A.P. DeFonzo, IEEE J. Quantum Electron., QE-16 pp. 277-288 (1980).
4. A. M. Vaucher, C. D. Striffler, Chi H. Lee, to be published in IEEE Trans. special issue of Millimeter-Waves, MTT-31, (1983).
5. E. A. J. Marcatili, Bell Syst. Tech. J., Vol. 48, pp. 2079-2102 (1969).
6. M. G. Li, W. L. Cao, V. K. Mathur, Chi H. Lee, Electron Lett., Vol 18 No. 11,pp.454-456 (1982).
7. A. M. Vaucher, M.G. Li, Chi H. Lee, Electron. Lett. Vol 18 No. 25/26 pp 1066-1067 (1982).
8. Chi H. Lee, A. Antonetti, G. Mourou, Opt. Commun., 21, pp. 158-161 (1977).